WDR26 Haploinsufficiency Causes a Recognizable Syndrome of Intellectual Disability, Seizures, Abnormal Gait, and Distinctive Facial Features

Cara M. Skraban,[1,2] Constance F. Wells,[3] Preetha Markose,[1] Megan T. Cho,[4] Addie I. Nesbitt,[5] P.Y. Billie Au,[6] Amber Begtrup,[4] John A. Bernat,[7] Lynne M. Bird,[8] Kajia Cao,[5] Arjan P.M. de Brouwer,[9,10] Elizabeth H. Denenberg,[5] Ganka Douglas,[4] Kristin M. Gibson,[5] Katheryn Grand,[1] Alice Goldenberg,[11] A. Micheil Innes,[6] Jane Juusola,[4] Marlies Kempers,[9] Esther Kinning,[12] David M. Markie,[13] Martina M. Owens,[14] Katelyn Payne,[15] Richard Person,[4] Rolph Pfundt,[9] Amber Stocco,[16] Claire L.S. Turner,[17] Nienke E. Verbeek,[18] Laurence E. Walsh,[15] Taylor C. Warner,[7] Patricia G. Wheeler,[19] Dagmar Wieczorek,[20] Alisha B. Wilkens,[1,5] Evelien Zonneveld-Huijssoon,[18] Deciphering Developmental Disorders Study,[21] Tjitske Kleefstra,[9,10] Stephen P. Robertson,[3] Avni Santani,[5,22] Koen L.I. van Gassen,[18] and Matthew A. Deardorff[1,2,*]

We report 15 individuals with de novo pathogenic variants in *WDR26*. Eleven of the individuals carry loss-of-function mutations, and four harbor missense substitutions. These 15 individuals comprise ten females and five males, and all have intellectual disability with delayed speech, a history of febrile and/or non-febrile seizures, and a wide-based, spastic, and/or stiff-legged gait. These subjects share a set of common facial features that include a prominent maxilla and upper lip that readily reveal the upper gingiva, widely spaced teeth, and a broad nasal tip. Together, these features comprise a recognizable facial phenotype. We compared these features with those of chromosome 1q41q42 microdeletion syndrome, which typically contains *WDR26*, and noted that clinical features are consistent between the two subsets, suggesting that haploinsufficiency of *WDR26* contributes to the pathology of 1q41q42 microdeletion syndrome. Consistent with this, *WDR26* loss-of-function single-nucleotide mutations identified in these subjects lead to nonsense-mediated decay with subsequent reduction of RNA expression and protein levels. We derived a structural model of WDR26 and note that missense variants identified in these individuals localize to highly conserved residues of this WD-40-repeat-containing protein. Given that *WDR26* mutations have been identified in ~1 in 2,000 of subjects in our clinical cohorts and that *WDR26* might be poorly annotated in exome variant-interpretation pipelines, we would anticipate that this disorder could be more common than currently appreciated.

Characterizing and identifying syndromic forms of intellectual disability can be difficult for both clinicians and scientists. This is typically due to variability in the severity, associated features, and rarity of these disorders. Several of these challenges have improved with the advent of genome-wide sequencing coupled with careful standardized phenotyping and highly collaborative networks, which have markedly facilitated the identification, characterization, and recognition of rare syndromic disorders with intellectual disability. However, limitations often related to poor annotation or understanding of gene function continue to hinder the identification of disease-related genes. Here, we report the recognition of a role for *WDR26* (WD40 repeat protein 26 [MIM: 617424]) in human syndromic intellectual disability. This recognition was dependent upon the presence of de novo variants, the utilization of broad reference datasets that included this variably annotated gene, and a concerted effort of international collaborators to identify individuals and characterize the clinical features.

In the evaluation of two individuals (1 and 2) with mildly dysmorphic features and intellectual disability at different institutions (GeneDx, Children's Hospital of Philadelphia, and University Medical Center Utrecht),

[1]Division of Genetics, Children's Hospital of Philadelphia, Philadelphia, PA 19104, USA; [2]Department of Pediatrics, Perelman School of Medicine, University of Pennsylvania, Philadelphia, PA 19104, USA; [3]Clinical Genetics Group, Department of Women's & Children's Health, Dunedin School of Medicine, University of Otago, Dunedin 9054, New Zealand; [4]GeneDx, Gaithersburg, MD 20877, USA; [5]Division of Genomic Diagnostics, Children's Hospital of Philadelphia, Philadelphia, PA, 19104 USA; [6]Department of Medical Genetics and Alberta Children's Hospital Research Institute, Cumming School of Medicine, University of Calgary, Calgary, AB T2N1N4, Canada; [7]Division of Medical Genetics, Stead Family Department of Pediatrics, University of Iowa, Iowa City, IA 52242, USA; [8]Department of Pediatrics, University of California, San Diego and Rady Children's Hospital, San Diego, CA 92123, USA; [9]Department of Human Genetics, Radboud University Medical Centre, 6500 HB Nijmegen, the Netherlands; [10]Donders Institute for Brain, Cognition, and Behaviour, Radboud University Medical Centre, 6500 HB Nijmegen, the Netherlands; [11]Service de Génétique, Centre Hospitalier Universitaire de Rouen, Centre Normand de Génomique Médicale et Médecine Personnalisée, 76031 Rouen, France; [12]West of Scotland Genetics Service, Queen Elizabeth Hospitals, Glasgow, Scotland G51 4TF, UK; [13]Department of Pathology, Dunedin School of Medicine, University of Otago, Dunedin 9054, New Zealand; [14]Molecular Genetics Department, Royal Devon and Exeter NHS Foundation Trust, Barrack Road, Exeter EX2 5DW, UK; [15]Division of Child Neurology, Riley Hospital for Children, Indiana University Health Physicians, Indianapolis, IN 46202, USA; [16]INTEGRIS Baptist Child Neurology Clinic, Oklahoma City, OK 73112, USA; [17]Peninsula Clinical Genetics Service, Royal Devon and Exeter Hospital, Exeter EX1 2ED, UK; [18]Department of Genetics, University Medical Center Utrecht, 3508 AB Utrecht, the Netherlands; [19]Division of Genetics, Arnold Palmer Hospital, Orlando, FL 32806, USA; [20]Institut für Humangenetik, Universitätsklinikum Düsseldorf, Heinrich-Heine-Universität, 40225 Düsseldorf, Germany; [21]Wellcome Trust Sanger Institute, Wellcome Trust Genome Campus, Hinxton, Cambridge CB10 1SA, UK; [22]Department of Pathology, Perelman School of Medicine, University of Pennsylvania, Philadelphia, PA 19104 USA
*Correspondence: deardorff@email.chop.edu
http://dx.doi.org/10.1016/j.ajhg.2017.06.002.

Table 1. Pathogenic *WDR26* Variants

Individual	cDNA Notation (GenBank: NM_025160.6)	Predicted Effect on Protein (GenBank: NP_079436.4)	Inheritance
1	c.1276G>T	p.Glu426*	de novo
2	c.1161_1162del	p.His389Profs*6	de novo
3	c.1457del	p.Val486Glufs*9	de novo
4	c.644T>C	p.Leu215Pro	de novo
5	c.904_905del	p.Gln302Aspfs*22	de novo
6	c.850G>A	p.Asp284Asn	de novo
7	c.137C>A	p.Ser46*	de novo
8	c.1570C>T	p.Gln524*	de novo
9	c.762T>G	p.Ser254Arg	de novo
10	c.1284G>A	p.Trp428*	de novo
11	c.1419+2dupT	splice site	de novo
12	c.835C>T	p.Arg279*	de novo
13	c.574dupA	p.Ile192Asnfs*8	de novo
14	c.514T>A	p.Trp172Arg	de novo
15	c.1149_1158+1del	p.Val384fs	de novo

each was noted to have a de novo nonsense mutation in the minimally characterized gene *WDR26*. Although this gene was not included in the OMIM gene set until recently (added March 31, 2017), it is included in Agilent v.4 and later exome capture sets (Agilent) as part of the RefSeq gene set.[1] The probability of loss-of-function intolerance (pLI)[2] for *WDR26* in the Exome Aggregation Consortium (ExAC) Browser was 1.00, strongly supporting that these variants are pathogenic. Subsequently, *WDR26* was included in lab gene annotation datasets that enabled the identification of additional de novo loss-of-function and missense variants (ExAC missense Z score for 68 observed and 175 expected: $Z = 3.94$[2]). Identification of additional subjects with *WDR26* variants was subsequently facilitated by the use of GeneMatcher,[3] PhenomeCentral,[4] and DECIPHER[5] as part of the Matchmaker Exchange Repositories.[6] We consequently identified 15 subjects with pathogenic variants of *WDR26*. All mutations were de novo, identified via trio exome sequencing, and included five frameshift, five nonsense, one splice site, and four missense mutations (Table 1). Individuals were identified in cohorts of 28,700 exomes for all indications and in 21,400 exomes for individuals with intellectual disability, giving a frequency of ~1 in 2,000 for all exome analyses and ~1 in 1,500 for individuals with intellectual disability.

To compare and characterize the clinical features of these individuals, we obtained consent and collected clinical information. Consent for publication was obtained for all photographs included in this manuscript. All individuals for whom evaluation or analysis beyond routine clinical care was performed were enrolled in a protocol with informed consent approved by the institutional review board of the Children's Hospital of Philadelphia, the Commissie Mensgebonden Onderzoek Regio Arnhem-Nijmegen, the Rouen University Hospital, the Health and Disability Ethics Committee of New Zealand, the East of England – Cambridge South of the National Research Ethics Service for the Deciphering Developmental Disorders (DDD) UK study, or the UK research ethics committee (REC) (10/H0305/83 granted by the Cambridge South REC and GEN/284/12 granted by the Republic of Ireland REC). A clinical case report for each subject is included in the Supplemental Note. Detailed molecular and clinical features for each individual have been compiled in Table S1.

The 15 subjects (10 females and 5 males) range in age from 24 months to 34 years. Consistent phenotypic features of these individuals include variable developmental delay, seizures, and similar facial features (Tables 2 and S1). Developmental delay ranges from mild to severe, and all individuals have delayed speech; four individuals had absent speech at the time of assessment (two at 4 years, one at 5.5 years, and one at 8 years). Individual 2, the oldest individual in the cohort, is described as having dysarthric speech as an adult. Motor delay is also common, such that the emergence of walking was reported from 17 months to 3 years. Of the ten individuals with available descriptions, all were described as having a wide-based, spastic, hemiparetic, and/or stiff-legged gait. Several subjects have stereotypies, including rocking behavior and abnormal hand movements or posturing, and overall, individuals are described as happy and socially engaging. Neurologic abnormalities are also common among the subjects. All individuals have a history of seizures, including febrile and/or non-febrile seizures, and several required antiepileptic medications for a period of time. The reported non-febrile seizure types include tonic-clonic, absence, and Rolandic, and age of onset ranges from the newborn period to 7 years. Minor structural brain malformations are present in 9 of 13 individuals. One female (individual 14) had a markedly abnormal left supratentorial hemispheric structure and has now had a left hemispherectomy with resulting hemiparesis. Hypotonia, often noted to be mild, was described in 9 of 12 individuals for whom information was available.

Individuals with mutations in *WDR26* also share a set of identifiable facial features (Figures 1 and S1). Common features include a prominent maxilla and upper lip (13/15), wide mouth (10/15), abnormal gingiva (9/15), widely spaced teeth (13/15), mildly coarse facial features (12/15), and a broad or full nasal tip (11/15). The gingival display represents a relatively unique finding (see individual 10 in Figure 1), but with the current relatively small number of individuals, it's unclear whether this represents increased vertical height of the maxilla or an inferiorly displaced attachment of the maxillary gingiva. This feature is an isolated finding in 7/15 individuals and manifests with overt gingival hyperplasia in an additional two individuals. Other facial features include anteversion of the nares

Table 2. Common Facial Features of Individuals with *WDR26* Mutations and 1q41 Microdeletions

Features	*WDR26* (n = 15)	1q41q42 Microdeletions Including *WDR26* (n = 17)
Developmental delay or intellectual disability	15/15	15/15
Seizures	15/15	13/14
CNS structural anomalies	10/14	11/15
Hypotonia	9/12	5/15
Abnormal gait	9/9	1/15
Happy and/or friendly personality	10/11	2/2
Autistic and/or repetitive behaviors or posturing	5/9	1/1
Coarse facial features	12/15	12/16
Full cheeks as a child	11/13	7/8
Abnormal eyebrows	6/15	5/12
Depressed nasal root	5/15	11/15
Anteverted nares	8/15	9/13
Full nasal tip	11/15	9/14
Prominent maxilla and protruding upper lip	13/15	7/12
Decreased cupid's bow	11/15	10/12
Widely spaced teeth	13/15	7/8
Abnormal gums	9/15	6/6

Fractions indicate the number observed over the number reported or ascertained. The following abbreviation is used: CNS, central nervous system.

(8/15), a tendency toward full cheeks in childhood (11/13), sparse lateral eyebrows (6/15), subjectively large irises often with rounded palpebral fissures (10/15), a depressed nasal bridge (5/15), mild micrognathia (5/15), and a partially flattened or decreased Cupid's bow of the upper vermillion border (11/15). Ophthalmologic abnormalities include strabismus and/or amblyopia (9/14) and Marcus Gunn jaw winking (1/15). Two individuals have small structural cardiac defects (one with a right sided aortic arch and one with a ventricular septal defect). One individual (individual 10) has a cleft palate. No subjects have major structural defects of the respiratory or gastrointestinal systems. Six individuals have been described as having feeding difficulties and/or failure to thrive. Although skeletal findings were ascertained in only a minority of subjects, one (individual 8) was found to have osteopathia striata of the distal femurs, two have pes cavus (individuals 9 and 11), one has moderate forefoot varus and mild left hip dysplasia (individual 13), and two have mild contractures of the lower extremities (knees in individual 8 and knees and hips in individual 10).

WDR26 is located in chromosomal region 1q42, which is proposed to be implicated in 1q41q42 microdeletion syndrome.[7] The findings of individuals with 1q42 deletions are characterized by consistent facial features, developmental delay, and a predisposition for seizures. Other clinical features in some individuals include short stature, microcephaly, and multiple structural anomalies including cleft palate, clubfoot, congenital heart disease, and congenital diaphragmatic hernia.[7–14] Deletions for these subjects range in size from 300 kb to 10 Mb and include varied subsets of genes. However, somewhat strikingly, a comparison of the clinical and facial features of subjects with minimal microdeletions, as noted in additional photos of individual 16 (Figure 1) from Au et al.[15] and the subject reported in Cassina et al.,[16] and of subjects with isolated *WDR26* mutations demonstrates a nearly complete overlap.

This overlap between clinical features of individuals with *WDR26* variants and those seen with 1q4142 microdeletions suggests that both result from haploinsufficiency of *WDR26*. However, it is formally possible that the missense, nonsense, and frameshift variants identified could lead to a dominant-negative protein. Furthermore, very little is known about the regulation of *WDR26* mRNA, which raises the possibility that *WDR26* nonsense or truncating mutations could occur in a stable mRNA and lead to the formation of a truncated, dominant-negative protein. To rigorously test these possibilities, we performed several experiments. First, because nonsense and frameshift mutations often lead to nonsense-mediated decay of mutant mRNA,[17,18] we tested the stability of mutant mRNA in each of three available lymphoblastoid cell lines derived from subjects with de novo *WDR26* mutations (individuals 2, 5, and 6), along with two control samples. In comparison to the equal presence of mutant and wild-type alleles in genomic DNA (Figure 2A, top row), the mutant allele was markedly reduced in cDNA derived from untreated cell lines with frameshift mutations (Figure 2A, middle row, two left panels). Because

Figure 1. Clinical Features of Individuals with Pathogenic *WDR26* Variants
Each individual is noted with a number that corresponds to that used throughout the manuscript. Images are clustered for each individual. Included on the top left of each cluster is the variant identified, the sex, and an additional study identifier, also noted in Table S1 at the right.

cycloheximide (CHX) is an inhibitor of nonsense-mediated decay of mRNA, we also treated the cell lines with cycloheximide before production of cDNA. With this treatment, we observed stabilization of the mutant mRNA allele (Figure 2A, bottom row, two left panels), consistent with nonsense-mediated decay in cycloheximide-untreated cells. We also observed no truncated WDR26 in any of the cell lines with western blotting (data not shown). We noted that, in contrast to the frameshift alleles, the missense mutation (c.850G>A, predicted to encode p.Asp284Asn) did not exhibit loss of expression of the mutant allele in the absence of cycloheximide, consistent with the expected absence of nonsense-mediated decay and suggesting an alternative mechanism of pathogenicity. Second, to assess whether this nonsense-mediated decay leads to a reduction in *WDR26* mRNA, as would be expected for haploinsufficiency, we performed quantitative RT-PCR of total *WDR26* mRNA levels from these same cell lines. These data demonstrated significant reductions for the frameshift mutations but only a

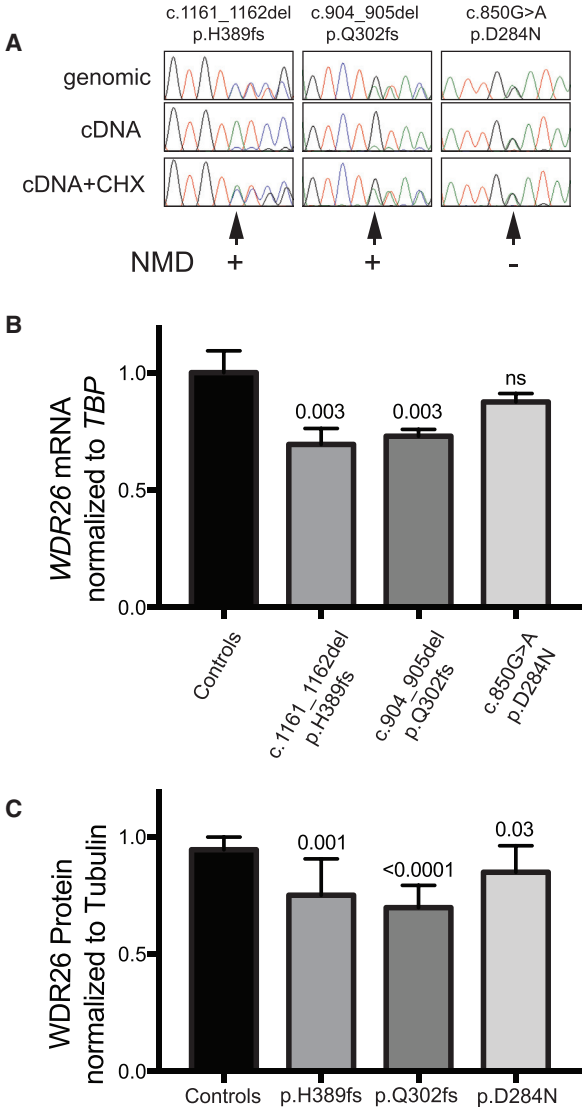

Figure 2. Effect of *WDR26* Mutations on Nonsense-Mediated RNA Decay and Protein Levels

(A) Nonsense-mediated mRNA decay (NMD) analysis. Epstein-Barr-virus-immortalized lymphoblastoid cell lines (LCLs) from subject 2 (c.1161_1162del [p.His389Profs*6], labeled p.H389fs), subject 4 (c.644T>C [p.Gln302Aspfs*22], labeled p.Q302fs), and subject 6 (c.850G>A [p.Asp284Asn], labeled p.D284N) were cultured in the presence of 1 mg/mL cycloheximide (CHX) for 6 hr and analyzed by RT-PCR and sequencing for the presence of wild-type and mutant alleles. Sequencing chromatograms for heterozygous genomic DNA as reference, untreated, and CHX-treated conditions are shown, demonstrating the reduced presence of the frameshift alleles but not the missense allele, denoted by an arrow at the location of the mutation and summarized result of the NMD assay (+ or −).

(B) *WDR26* RNA expression levels. Consistent with (A), digital droplet-based quantitative RT-PCR of *WDR26* mRNA expression normalized to TBP mRNA demonstrated a statistically significant reduction of expression for the frameshift alleles (69% for c.1161_1162del and 73% for c.644T>C) but not for the c.850G>A missense allele (88%).

(C) WDR26 levels were quantified by fluorescent western blotting and normalized to tubulin. Significantly lower WDR26 levels than control levels were noted for each pathogenic allele tested (75% for p.His389Profs*6, 70% for p.Gln302Aspfs*22, and 85% for p.Asp284Asn). The mean and SEM, along with unpaired two-tailed p values comparing multiple biological replicates (three for RNA and seven for protein) with controls, are demonstrated for each condition.

non-significant trend for the c.850G>A missense mutation (Figure 2B), suggesting a possible alternative pathogenic mechanism for missense variants. Lastly, to assess the effect of these variants on total protein levels, we performed quantitative western blotting with normalization to tubulin (Figure 2C). This demonstrated strongly significant reductions in WDR26 levels for the frameshift alleles and a mild reduction for the p.Asp284Asn missense variant (Figure 2C). Together, these data confirm that clinical features most likely arise from WDR26 haploinsufficiency and suggest that WDR26 missense variants could alter protein stability and also lead to reduced function in a manner consistent with deletion and loss-of-function alleles.

To further explore the mechanism of pathogenicity for the de novo *WDR26* missense variants, we assessed their conservation and localization within the protein. WDR26, typical for this protein class, contains WD-40 repeats (Figure 3A) and conserved LisH (LIS1 homology) and CTLH (C-terminal LIS homology) domains.[19,20] Each of the de novo missense WDR26 variants is located within a region of high sequence phylogenetic conservation (Figure 3B) and in one of these key motifs. Residues Trp172 and Leu215 are identical phylogenetically through *Drosophila*, whereas more notably, both Ser254 and Asp284 are identically conserved through yeast. This suggests that even subtle changes at these sites would be poorly tolerated. Consistent with this, the ExAC Residual Variance Intolerance Score (ExAC RVIS) for WDR26 is 18.1%,[21] and the subRVIS for the domains containing amino acids 172, 215, 254, and 284 is 9.2% (guidelines state that less than 35% is not tolerated[22]). Also consistently, the residue-specific prediction algorithms SIFT, PROVEAN, PolyPhen-2, and MutationTaster all predict the p.Trp172Arg, p.Leu215Pro, and p.Ser254Arg variants to be damaging. Finally, although there are mixed results for the informatics assessment of p.Asp284Asn, which alters the charge for a residue identically conserved through yeast, it is predicted to be damaging by PROVEAN and MutationTaster.

To better understand the potential effect of the missense variants identified in these subjects, we modeled a structure for WDR26 on the solved crystal structure for *Drosophila* WDS (PDB: 4CY3),[23] a homolog of human WDR5 in humans and a closely related WDR protein. In contrast with previous primary-sequence-based domain calling approaches, which suggest that WDR26 contains five, six, or seven WD-40 repeats,[19,20,24–26] our model for WDR26 suggests that it contains 14 variably perfect WD-40 repeats, each of which forms four-stranded anti-parallel β sheets or blades, and together they all compose two seven-bladed complete β propeller structures (Figures 3A and 3C). WD-40 domains 1–7 (WD1–WD7, amino acids 1–353) comprise an N-terminal β propeller,

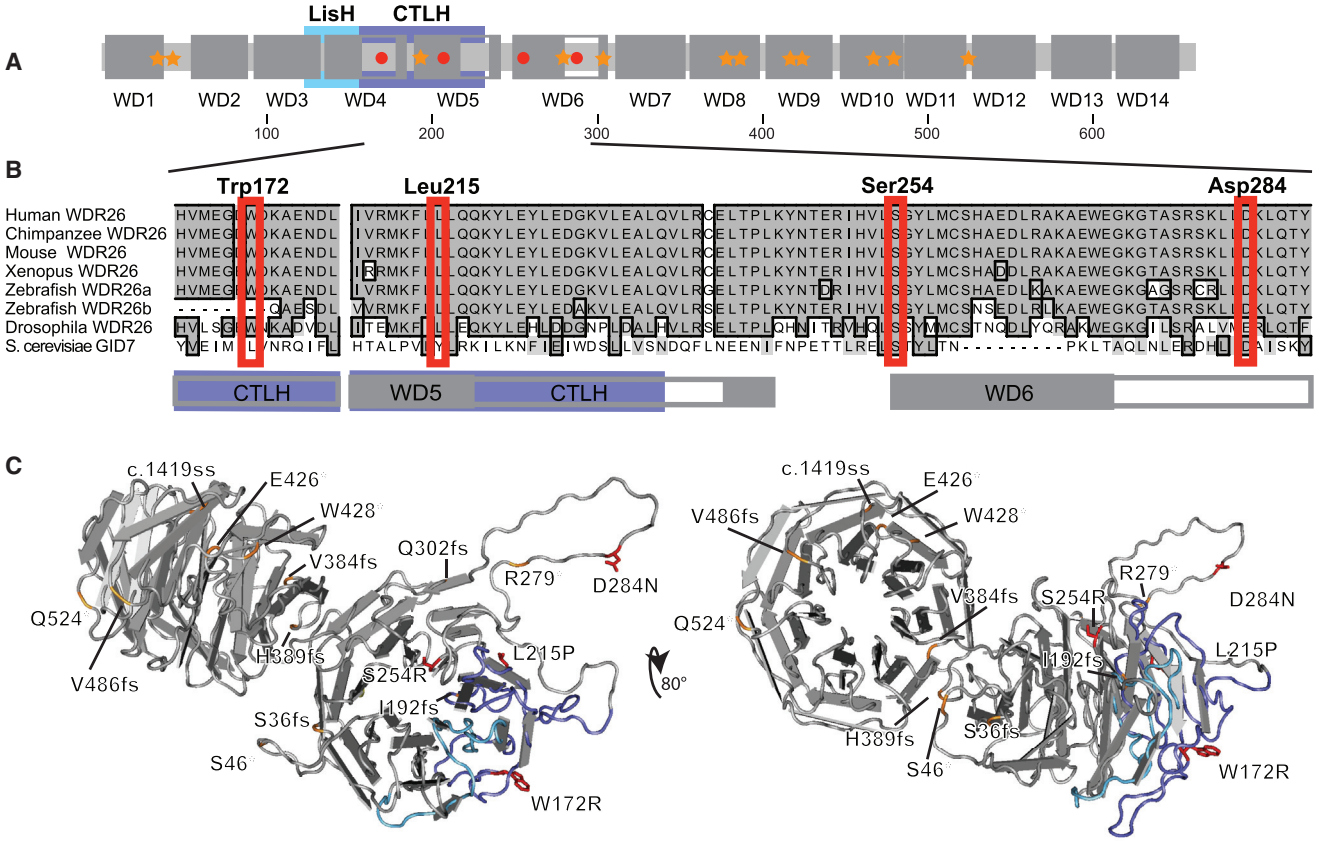

Figure 3. Localization of WDR26 Variants

(A) Schematic domains of WDR26. Illustrated are the key domains of WDR26, which include the 14 deduced WD repeats (larger dark-gray boxes labeled WD1–WD14; insertions in the domains are noted by unfilled gray bordered segments), the LisH and CTLH homology domains (in aqua and purple, respectively), and the location of loss-of-function (orange stars) and missense (red circles) variants. Scale numbers demonstrating amino acid residues are indicated beneath.

(B) Localization of WDR26 missense variants to highly conserved residues in WD repeats near the CTLH domain. ClustalW homology alignments for human WDR26a (UniProtKB: Q9H7D7; GenBank: NP_079436.4), Chimpanzee (*Pan troglodytes*) WDR26 (UniProtKB: K7CSM5), mouse (*Mus musculus*) WDR26 (UniProtKB/Swiss-Prot: Q8C6G8.3), frog (*Xenopus laevis*) WDR26 (UniProtKB: A0A0H5BJW1), zebrafish (*Danio rerio*) WDR26a (GenBank: NP_001189371.1) and predicted WDR26b (GenBank: XP_001921656.4), fruit fly (*Drosophila melanogaster*) WDR26 (UniProtKB/Swiss-Prot: Q7K0L4.1), and yeast (*Saccharomyces cerevisiae* S288c) GID7 (UniProtKB/Swiss-Prot: P25569.2) are shown. Identical residues are in dark gray with a black outlined border. Similar residues are indicated with light-gray shading and no border. Mutated residues are noted above, and red boxes denote the position in all species. Gray and purple boxes beneath denote the WD and CTLH domain boundaries, respectively.

(C) Structural model of WDR26 with variants. Illustrated are structural models of WDR26 with a direct view of the N-terminal β propeller domain (left) and an ~80° rotation toward the viewer to directly show the C-terminal β propeller domain (right). β sheets are illustrated as flat directional arrows. Note the organization of four β sheets into WD modules. The LisH and CTLH domains are noted by aqua and purple shading, respectively, of the protein backbone. Locations of variants are labeled and indicated; missense mutations are indicated by red shading of the residue and sidechain, and the relative position of loss-of-function alleles is noted by orange shading of the protein backbone.

and WD8–WD14 (amino acids 354–645) comprise a C-terminal β propeller. The C-terminal β propeller is ~80° off-axis from the N-terminal β propeller and contains the conserved LisH and CTLH domains (Figure 3C shows two views to illustrate each β propeller). Consistent with key functional roles, p.Trp172Arg (individual 14) and p.Leu215Pro (individual 4) lie within the CTLH domain, and p.Leu215Pro lies in the WD5 repeat in a key β sheet residue. Similarly, p.Ser254Arg (individual 9) lies in the neighboring WD6 repeat at the edge of a β sheet. The locations of these variants suggest that alterations in β sheets, which comprise essential components of the WD repeats, result in peptides with abnormal function and/or instability of the β propeller motif. In comparison, p.Asp284Asn (individual 6) lies within a predicted loop that is less well structured and extends from the surface of the protein to lie outside of the β propeller structure. In combination with the localization of this variant, the very high conservation of this region (Figure 3B), along with data suggesting that functional specificity of WD-40 proteins is determined by domains that extend from the β propeller,[27] suggests that the Asp284 residue could be involved in key extrinsic interactions. This also suggests that protein stability might be more tolerant of alteration at this site, a finding noted above by western blotting of WDR26 from the lymphoblastoid cells from this

Table 3. Growth Parameters for Individuals with *WDR26* Mutations

Parameter	n	Average (*Z* Score)	Range (*Z* Score)	No. Abnormal (No. < *Z* Score)
Birth weight	13	−0.9	−2.0 to 1.8	4/13 ≤ −1.5
Later Time Point				
Length	15	−0.6	−4.0 to 1.4	2/15 ≤ −1.5
Weight	14	−0.9	−5.0 to 4.3	6/14 ≤ −1.5
OFC	14	−0.9	−3.0 to 1.1	3/14 ≤ −1.5

Fractions indicate the number observed over the number reported or ascertained. The following abbreviation is used: OFC, occipital-frontal circumference.

individual (Figure 2C). The finding of similar clinical features of individuals with 1q41q42 microdeletions, loss-of-function nonsense and frameshift mutations, and missense mutations suggests that the missense variants identified in these individuals disrupt a key function of WDR26.

In total, we have identified 15 subjects with mutations that result in haploinsufficiency of *WDR26*. Because of the location of *WDR26* within the 1q41q42 deletion syndrome region, it might have been considered a candidate gene for causing the similar clinical features noted in these individuals. Of note, these microdeletions range in size from 300 kb to 10 Mb and include a varied subsets of genes; in fact, several attempts have been made to identify potential candidate genes for the clinical features seen in these individuals.[7–16] More recently, two papers[15,16] described individuals with intellectual disability, seizures, and dysmorphic features with 590 and 286 kb deletions on 1q41q42 that included *FBXO28* (MIM: 609100) and *WDR26*, along with *DEGS1* (MIM: 615843), *NVL* (MIM: 602426), *MIR320B2*, *CNIH4* (MIM: 617483), *MIR4742*, and *CNIH3* (Figure S2). Each concluded that, along with previously published cases, this narrowed the region of overlap to include a single candidate gene, *FBXO28*. However, these and previous analyses relied on the observation by Shaffer et al.[7] that *WDR26* was excluded from the smallest region of overlap by a single individual (subject 5). When reviewing this case in light of our current recognition of a facial phenotype associated with isolated *WDR26* mutations (Figures 1 and S1 and Tables 2, 3, and S1), we found that this individual lacks the characteristic facial features. Given that he has a large (5.1 Mb) deletion, it is likely that his associated features are due to haploinsufficiency of other genes. Furthermore, the ExAC pLI of 1.0 and constraint for missense variants of $Z = 3.94$ for *WDR26* are consistent with a very strong effect if deleted, whereas the pLI for *FBXO28* is less significant at 0.93, and all other genes in this interval demonstrate pLIs less than these. Together, when assessing both neurocognitive and facial phenotypes, these genetic data support that *WDR26* is the likely candidate gene whose haploinsufficiency is the cause of 1q41q42 deletion syndrome.

Assessment of the mechanism by which *WDR26* haploinsufficiency leads to human developmental disorders has yet to be elucidated. *WDR26* is expressed in most human tissues, including the brain and skeletal muscle at both fetal and adult stages,[19] consistent with the tissues involved in individuals with *WDR26* mutations. However, multiple roles have been proposed for WDR26. Data from relatively few studies suggest that it could play wide-ranging roles in regulation of MAPK, Wnt, and PI3K signaling; neuronal and cardiomyoblast proliferation; apoptosis signaling; and leukocyte activation and signaling.[19,20,24–26,28–30] We have tested cell lines derived from heterozygous subjects for evidence of altered Wnt signaling but have not noted any changes in lymphoblastoid or fibroblast cell types (data not shown).

Similarly, additional understanding of the biological function of WDR26 could indeed benefit from insight gained from clinical features of individuals with *WDR26* mutations. For example, the observed common features (including intellectual disability more prevalently involving speech; seizures; wide-based, spastic, and/or stiff-legged gait; a prominent maxilla and upper lip; and widely spaced teeth; Tables 2 and S1) could underlie the reasons that several alternative diagnoses were considered for individuals in this cohort. Considered diagnoses included Angelman syndrome (MIM: 105830; individuals 4, 7, 10, and 11) and Pitt-Hopkins syndrome (MIM: 610954; individual 4), suggesting a disorder of neuronal development.[31] In addition, atypical Cornelia de Lange syndrome (MIM: 122470; individuals 1 and 6), Coffin-Siris syndrome (MIM: 135900; individual 1), Floating-Harbor syndrome (MIM: 136140; individual 6), X-linked alpha-thalassemia/mental retardation syndrome (MIM: 301040; individuals 7, 9, and 15), Kabuki syndrome (MIM: 147920; individual 13), and Kleefstra syndrome (MIM: 610253; individuals 12 and 15) were considered. These diagnoses suggest that additional possible pathogenic mechanisms for *WDR26* haploinsufficiency might be related to chromatin regulation.[32–37] This would be consistent with an overlap between the clinical features in these subjects and those of the recently denoted "transcriptomopathies."[38,39]

In summary, we coupled exome sequencing with variant annotation and interpretation via pipelines including broadly annotated gene sets, along with global collaborative tools, to identify human mutations in *WDR26*. This cohort of individuals demonstrates a recognizable phenotype of intellectual disability, developmental delay, seizures,

abnormal gait, and characteristic facial features that include a prominent maxilla and upper lip that readily reveal the upper gingiva and widely spaced teeth. Notably, this gene, although included in most exome capture sets, it is not included in some database gene analysis sets. We would suggest that if a *WDR26* mutation is suspected in an individual on the basis of clinical features, previous exome data could be reanalyzed. Given the phenotypic and mechanistic overlap of haploinsufficiency, *WDR26* is most likely the major contributory gene in 1q41q42 deletion syndrome as a major factor in the neurocognitive and facial phenotypes. Finally, although little is known to date about its function, we anticipate that reduced expression of *WDR26* alters multiple signaling pathways and cellular mechanisms to result in this recognizable human phenotype.

Supplemental Data

Supplemental Data include a Supplemental Note, two figures, and one table and can be found with this article online at http://dx.doi.org/10.1016/j.ajhg.2017.06.002. Detailed experimental methods are available upon request.

Conflicts of Interest

M.T.C., A.B., G.D., J.J., and R.P. are employees of GeneDx.

Acknowledgments

We are exceptionally grateful to the individuals and families who participated in this study; colleagues who contributed samples and clinical information, including Dr. John Tolmie; and Harriet Saunders for technical assistance. This work was supported by institutional funds from the Children's Hospital of Philadelphia Research Institute to C.M.S. and M.A.D. and from CureKids New Zealand to S.P.R. The authors would like to thank the Exome Aggregation Consortium and the groups that provided exome variant data for comparison. We acknowledge the Deciphering Developmental Disorders study, which presents independent research commissioned by the Health Innovation Challenge Fund (grant HICF-1009-003), a parallel funding partnership among the Wellcome Trust, Department of Health, and Wellcome Trust Sanger Institute (grant WT098051). The views expressed in this publication are those of the authors and not necessarily those of the Wellcome Trust or the Department of Health. The research team acknowledges the support of the National Institute for Health Research through the Comprehensive Clinical Research Network.

Received: January 24, 2017
Accepted: May 30, 2017
Published: July 6, 2017

Web Resources

BLASTP, https://blast.ncbi.nlm.nih.gov/Blast.cgi?PAGE=Proteins
Combined Annotation Dependent Depletion (CADD), http://cadd.gs.washington.edu/home
DECIPHER, https://decipher.sanger.ac.uk
Elements of Morphology: Human Malformation Terminology, https://elementsofmorphology.nih.gov/
Exome Aggregation Consortium (ExAC) Browser, http://exac.broadinstitute.org
GenBank, https://www.ncbi.nlm.nih.gov/genbank/
GeneMatcher, https://genematcher.org/
Human Phenotype Ontology Browser, http://www.human-phenotype-ontology.org
Mutation Taster, http://www.mutationtaster.org/
OMIM, http://www.omim.org/
PolyPhen-2, http://genetics.bwh.harvard.edu/pph2/
PROVEAN, http://provean.jcvi.org/index.php
RCSB Protein Data Bank, http://www.rcsb.org/pdb/home/home.do
Residual Variation Intolerance Score (RVIS), http://genic-intolerance.org
SIFT, http://sift.jcvi.org
SubRVIS, http://www.subrvis.org
UniProtKB, http://www.uniprot.org/help/uniprotkb

References

1. Farrell, C.M., O'Leary, N.A., Harte, R.A., Loveland, J.E., Wilming, L.G., Wallin, C., Diekhans, M., Barrell, D., Searle, S.M., Aken, B., et al. (2014). Current status and new features of the Consensus Coding Sequence database. Nucleic Acids Res. *42*, D865–D872.
2. Lek, M., Karczewski, K.J., Minikel, E.V., Samocha, K.E., Banks, E., Fennell, T., O'Donnell-Luria, A.H., Ware, J.S., Hill, A.J., Cummings, B.B., et al.; Exome Aggregation Consortium (2016). Analysis of protein-coding genetic variation in 60,706 humans. Nature *536*, 285–291.
3. Sobreira, N., Schiettecatte, F., Valle, D., and Hamosh, A. (2015). GeneMatcher: a matching tool for connecting investigators with an interest in the same gene. Hum. Mutat. *36*, 928–930.
4. Buske, O.J., Girdea, M., Dumitriu, S., Gallinger, B., Hartley, T., Trang, H., Misyura, A., Friedman, T., Beaulieu, C., Bone, W.P., et al. (2015). PhenomeCentral: a portal for phenotypic and genotypic matchmaking of patients with rare genetic diseases. Hum. Mutat. *36*, 931–940.
5. Firth, H.V., Richards, S.M., Bevan, A.P., Clayton, S., Corpas, M., Rajan, D., Van Vooren, S., Moreau, Y., Pettett, R.M., and Carter, N.P. (2009). DECIPHER: Database of Chromosomal Imbalance and Phenotype in Humans Using Ensembl Resources. Am. J. Hum. Genet. *84*, 524–533.
6. Philippakis, A.A., Azzariti, D.R., Beltran, S., Brookes, A.J., Brownstein, C.A., Brudno, M., Brunner, H.G., Buske, O.J., Carey, K., Doll, C., et al. (2015). The Matchmaker Exchange: a platform for rare disease gene discovery. Hum. Mutat. *36*, 915–921.
7. Shaffer, L.G., Theisen, A., Bejjani, B.A., Ballif, B.C., Aylsworth, A.S., Lim, C., McDonald, M., Ellison, J.W., Kostiner, D., Saitta, S., and Shaikh, T. (2007). The discovery of microdeletion syndromes in the post-genomic era: review of the methodology and characterization of a new 1q41q42 microdeletion syndrome. Genet. Med. *9*, 607–616.
8. Filges, I., Röthlisberger, B., Boesch, N., Weber, P., Wenzel, F., Huber, A.R., Heinimann, K., and Miny, P. (2010). Interstitial deletion 1q42 in a patient with agenesis of corpus callosum: Phenotype-genotype comparison to the 1q41q42 microdeletion suggests a contiguous 1q4 syndrome. Am. J. Med. Genet. A. *152A*, 987–993.
9. Kantarci, S., Ackerman, K.G., Russell, M.K., Longoni, M., Sougnez, C., Noonan, K.M., Hatchwell, E., Zhang, X., Pieretti

Vanmarcke, R., Anyane-Yeboa, K., et al. (2010). Characterization of the chromosome 1q41q42.12 region, and the candidate gene DISP1, in patients with CDH. Am. J. Med. Genet. A. *152A*, 2493–2504.
10. Mazzeu, J.F., Krepischi-Santos, A.C., Rosenberg, C., Szuhai, K., Knijnenburg, J., Weiss, J.M., Kerkis, I., Mustacchi, Z., Colin, G., Mombach, R., et al. (2007). Chromosome abnormalities in two patients with features of autosomal dominant Robinow syndrome. Am. J. Med. Genet. A. *143A*, 1790–1795.
11. Rice, G.M., Qi, Z., Selzer, R., Richmond, T., Thompson, K., Pauli, R.M., and Yu, J. (2006). Microdissection-based high-resolution genomic array analysis of two patients with cytogenetically identical interstitial deletions of chromosome 1q but distinct clinical phenotypes. Am. J. Med. Genet. A. *140*, 1637–1643.
12. Rosenfeld, J.A., Lacassie, Y., El-Khechen, D., Escobar, L.F., Reggin, J., Heuer, C., Chen, E., Jenkins, L.S., Collins, A.T., Zinner, S., et al. (2011). New cases and refinement of the critical region in the 1q41q42 microdeletion syndrome. Eur. J. Med. Genet. *54*, 42–49.
13. Slavotinek, A.M., Moshrefi, A., Lopez Jiminez, N., Chao, R., Mendell, A., Shaw, G.M., Pennacchio, L.A., and Bates, M.D. (2009). Sequence variants in the HLX gene at chromosome 1q41-1q42 in patients with diaphragmatic hernia. Clin. Genet. *75*, 429–439.
14. Wat, M.J., Veenma, D., Hogue, J., Holder, A.M., Yu, Z., Wat, J.J., Hanchard, N., Shchelochkov, O.A., Fernandes, C.J., Johnson, A., et al. (2011). Genomic alterations that contribute to the development of isolated and non-isolated congenital diaphragmatic hernia. J. Med. Genet. *48*, 299–307.
15. Au, P.Y., Argiropoulos, B., Parboosingh, J.S., and Micheil Innes, A. (2014). Refinement of the critical region of 1q41q42 microdeletion syndrome identifies FBXO28 as a candidate causative gene for intellectual disability and seizures. Am. J. Med. Genet. A. *164A*, 441–448.
16. Cassina, M., Rigon, C., Casarin, A., Vicenzi, V., Salviati, L., and Clementi, M. (2015). FBXO28 is a critical gene of the 1q41q42 microdeletion syndrome. Am. J. Med. Genet. A. *167*, 1418–1420.
17. Chang, Y.F., Imam, J.S., and Wilkinson, M.F. (2007). The nonsense-mediated decay RNA surveillance pathway. Annu. Rev. Biochem. *76*, 51–74.
18. Kervestin, S., and Jacobson, A. (2012). NMD: a multifaceted response to premature translational termination. Nat. Rev. Mol. Cell Biol. *13*, 700–712.
19. Zhu, Y., Wang, Y., Xia, C., Li, D., Li, Y., Zeng, W., Yuan, W., Liu, H., Zhu, C., Wu, X., and Liu, M. (2004). WDR26: a novel Gbeta-like protein, suppresses MAPK signaling pathway. J. Cell. Biochem. *93*, 579–587.
20. Sun, Z., Tang, X., Lin, F., and Chen, S. (2011). The WD40 repeat protein WDR26 binds Gβγ and promotes Gβγ-dependent signal transduction and leukocyte migration. J. Biol. Chem. *286*, 43902–43912.
21. Petrovski, S., Gussow, A.B., Wang, Q., Halvorsen, M., Han, Y., Weir, W.H., Allen, A.S., and Goldstein, D.B. (2015). The Intolerance of Regulatory Sequence to Genetic Variation Predicts Gene Dosage Sensitivity. PLoS Genet. *11*, e1005492.
22. Gussow, A.B., Petrovski, S., Wang, Q., Allen, A.S., and Goldstein, D.B. (2016). The intolerance to functional genetic variation of protein domains predicts the localization of pathogenic mutations within genes. Genome Biol. *17*, 9.
23. Dias, J., Van Nguyen, N., Georgiev, P., Gaub, A., Brettschneider, J., Cusack, S., Kadlec, J., and Akhtar, A. (2014). Structural analysis of the KANSL1/WDR5/KANSL2 complex reveals that WDR5 is required for efficient assembly and chromatin targeting of the NSL complex. Genes Dev. *28*, 929–942.
24. Goto, T., Matsuzawa, J., Iemura, S., Natsume, T., and Shibuya, H. (2016). WDR26 is a new partner of Axin1 in the canonical Wnt signaling pathway. FEBS Lett. *590*, 1291–1303.
25. Zhao, J., Liu, Y., Wei, X., Yuan, C., Yuan, X., and Xiao, X. (2009). A novel WD-40 repeat protein WDR26 suppresses H2O2-induced cell death in neural cells. Neurosci. Lett. *460*, 66–71.
26. Wei, X., Song, L., Jiang, L., Wang, G., Luo, X., Zhang, B., and Xiao, X. (2010). Overexpression of MIP2, a novel WD-repeat protein, promotes proliferation of H9c2 cells. Biochem. Biophys. Res. Commun. *393*, 860–863.
27. Stirnimann, C.U., Petsalaki, E., Russell, R.B., and Müller, C.W. (2010). WD40 proteins propel cellular networks. Trends Biochem. Sci. *35*, 565–574.
28. Feng, Y., Zhang, C., Luo, Q., Wei, X., Jiang, B., Zhu, H., Zhang, L., Jiang, L., Liu, M., and Xiao, X. (2012). A novel WD-repeat protein, WDR26, inhibits apoptosis of cardiomyocytes induced by oxidative stress. Free Radic. Res. *46*, 777–784.
29. Sun, Z., Smrcka, A.V., and Chen, S. (2013). WDR26 functions as a scaffolding protein to promote Gβγ-mediated phospholipase C β2 (PLCβ2) activation in leukocytes. J. Biol. Chem. *288*, 16715–16725.
30. Ye, Y., Tang, X., Sun, Z., and Chen, S. (2016). Upregulated WDR26 serves as a scaffold to coordinate PI3K/ AKT pathway-driven breast cancer cell growth, migration, and invasion. Oncotarget *7*, 17854–17869.
31. Zweier, C., de Jong, E.K., Zweier, M., Orrico, A., Ousager, L.B., Collins, A.L., Bijlsma, E.K., Oortveld, M.A., Ekici, A.B., Reis, A., et al. (2009). CNTNAP2 and NRXN1 are mutated in autosomal-recessive Pitt-Hopkins-like mental retardation and determine the level of a common synaptic protein in Drosophila. Am. J. Hum. Genet. *85*, 655–666.
32. Rohatgi, S., Clark, D., Kline, A.D., Jackson, L.G., Pie, J., Siu, V., Ramos, F.J., Krantz, I.D., and Deardorff, M.A. (2010). Facial diagnosis of mild and variant CdLS: Insights from a dysmorphologist survey. Am. J. Med. Genet. A. *152A*, 1641–1653.
33. Kaiser, F.J., Ansari, M., Braunholz, D., Concepción Gil-Rodríguez, M., Decroos, C., Wilde, J.J., Fincher, C.T., Kaur, M., Bando, M., Amor, D.J., et al.; Care4Rare Canada Consortium; and University of Washington Center for Mendelian Genomics (2014). Loss-of-function HDAC8 mutations cause a phenotypic spectrum of Cornelia de Lange syndrome-like features, ocular hypertelorism, large fontanelle and X-linked inheritance. Hum. Mol. Genet. *23*, 2888–2900.
34. Deardorff, M.A., Wilde, J.J., Albrecht, M., Dickinson, E., Tennstedt, S., Braunholz, D., Mönnich, M., Yan, Y., Xu, W., Gil-Rodríguez, M.C., et al. (2012). RAD21 mutations cause a human cohesinopathy. Am. J. Hum. Genet. *90*, 1014–1027.
35. Nikkel, S.M., Dauber, A., de Munnik, S., Connolly, M., Hood, R.L., Caluseriu, O., Hurst, J., Kini, U., Nowaczyk, M.J., Afenjar, A., et al.; FORGE Canada Consortium (2013). The phenotype of Floating-Harbor syndrome: clinical characterization of 52 individuals with mutations in exon 34 of SRCAP. Orphanet J. Rare Dis. *8*, 63.

36. Ausió, J., Levin, D.B., De Amorim, G.V., Bakker, S., and Macleod, P.M. (2003). Syndromes of disordered chromatin remodeling. Clin. Genet. *64*, 83–95.
37. Schrier, S.A., Bodurtha, J.N., Burton, B., Chudley, A.E., Chiong, M.A., D'avanzo, M.G., Lynch, S.A., Musio, A., Nyazov, D.M., Sanchez-Lara, P.A., et al. (2012). The Coffin-Siris syndrome: a proposed diagnostic approach and assessment of 15 overlapping cases. Am. J. Med. Genet. A. *158A*, 1865–1876.
38. Yuan, B., Pehlivan, D., Karaca, E., Patel, N., Charng, W.L., Gambin, T., Gonzaga-Jauregui, C., Sutton, V.R., Yesil, G., Bozdogan, S.T., et al. (2015). Global transcriptional disturbances underlie Cornelia de Lange syndrome and related phenotypes. J. Clin. Invest. *125*, 636–651.
39. Izumi, K. (2016). Disorders of Transcriptional Regulation: An Emerging Category of Multiple Malformation Syndromes. Mol. Syndromol. *7*, 262–273.